ORIGINAL PAPER

Struvite nucleation and crystal growth kinetics from cattle liquid manure

Anna Stanclik[1] · Nina Hutnik[1] · Krzysztof Piotrowski[2] · Andrzej Matynia[1]

Abstract
Cattle liquid manure (CLM) in future may become excellent raw material for the solid mineral fertilizers production. Phosphates(V) recovery from CLM can be done, e.g. through reaction crystallization of sparingly soluble salts: magnesium and ammonium phosphate(V) hexahydrate $MgNH_4PO_4 \cdot 6H_2O$ (MAP, struvite) or/and calcium phosphates(V). The original kinetic calculations based on experimental test results concerning continuous reaction crystallization of sparingly soluble phosphates(V) from cattle liquid manure in a continuous laboratory DT MSMPR (Draft Tube, Mixed Suspension Mixed Product Removal) crystallizer with internal circulation of suspension driven by propeller stirrer are presented. Two kinetic models of continuous mass crystallization in MSMPR crystallizer: SIG (Size Independent Growth) and RE SDG (Rojkowski Exponential Size Dependent Growth) were adopted. Advantageous effects of: low pH (8.5), elongated mean residence time of suspension in a crystallizer (3600 s) and magnesium ions excess in relation to phosphate(V) ions concentration (1.2:1) on the process results were observed. Under the considered process conditions linear crystal growth rates of struvite were: G from 4.11×10^{-3} to 1.01×10^{-2} µm s^{-1} and G_∞ from 5.30×10^{-3} to 1.02×10^{-2} µm s^{-1}.

Keywords Cattle liquid manure (CLM) · Struvite · Continuous reaction crystallization · SIG MSMPR kinetic model · SDG MSMPR kinetic model · Phosphorus recycling

List of symbols

Symbols

a	Parameter in Eq. (5) and (6) µm^{-1}
ACP	Amorphous calcium phosphate, $Ca_3(PO_4)_2$
B	Nucleation rate m^{-3} s^{-1}
CLM	Cattle liquid manure
CV	Coefficient of (crystal size) homogeneity %
DCPD	Brushite or dicalcium phosphate dehydrate, $CaHPO_4 \cdot 2H_2O$
DT	Draft tube
G	Crystal linear growth rate µm s^{-1}
G_0	Crystal linear growth rate for nuclei µm s^{-1}
G_∞	Crystal linear growth rate for the largest crystals µm s^{-1}
HAP	Hydroxyapatite
MAP	Magnesium and ammonium phosphate(V) hexahydrate, struvite
MSMPR	Mixed suspension mixed product removal (crystallizer)
n	Population density m^{-1} m^{-3}
n_0	Nuclei population density m^{-1} m^{-3}
L	Crystal size µm
L_d	Crystal mode size µm
L_m	Crystal mean size µm
L_{max}	Maximal crystal size µm
L_{16}	Crystal size corresponding to 16 mass % undersize fraction in cumulative distribution µm
L_{50}	Median crystal size µm
L_{84}	Crystal size corresponding to 84 mass % undersize fraction in cumulative distribution µm
M_T	Solid phase content in suspension kg$_{solid}$ m^{-3}
OCP	Octacalcium phosphate, $Ca_4H(PO_4)_3 \cdot 2.5H_2O$
RE	Rojkowski exponential (kinetic model)

✉ Krzysztof Piotrowski
krzysztof.piotrowski@polsl.pl

1 Wroclaw University of Science and Technology, Faculty of Chemistry, Wybrzeze Wyspianskiego 27, 50–370 Wroclaw, Poland

2 Department of Chemical Engineering and Process Design, Silesian University of Technology, M. Strzody 7, 44–101 Gliwice, Poland

SDG	Size dependent growth (kinetic model)
SIG	Size independent growth (kinetic model)
TCP	Tricalcium phosphate, $Ca_3(PO_4)_2$
V	Volume dm^3
x_i	Mass fraction of crystals of mean fraction size L_i –
T	Temperature K

Greek Letters

τ	Mean residence time of suspension in a crystallizer s

Subscripts

t	Total
w	Working

Introduction

Cattle liquid manure (CLM) is used mainly as natural organic fertilizer; however, in nearest future it may be further converted and become excellent raw material for the solid mineral fertilizers production (Sommer et al. 2013; Rahman et al. 2014). Recovery of phosphates(V) from CLM may be realized, e.g. through reaction crystallization of sparingly soluble salts: magnesium ammonium phosphate(V) hexahydrate $MgNH_4PO_4·6H_2O$ (MAP, struvite) (Parsons 2001) or/and calcium phosphates(V) (Valsami-Jones 2001). Struvite precipitates after providing the solution containing phosphate(V) ions (like CLM) with substrates: magnesium (e.g. magnesium chloride) and ammonium (e.g. some ammonium salt) ions, followed by raising this solution's pH ($7 < pH < 11$) (Le Corre et al. 2009). In the presence of calcium ions in CLM (see Table 1) also calcium phosphates(V)

Table 1 Filtrate of cattle faeces and urine mixture (CLM) after modification of its original chemical composition (Kozik et al. 2015, 2016)

Component	Cattle liquid manure (CLM)
PO_4^{3-}	0.340
NH_4^+	0.28
Ca	0.120
Mg	0.087 (or 0.1044)
K	0.28
Na	0.12
Cu	3.3×10^{-4}
Fe	2.3×10^{-4}
Mn	15.0×10^{-4}
Mo	0.1×10^{-4}
Zn	18×10^{-4}
Feed pH	5.8 (5.7)

Molar proportion PO_4^{3-}: Mg^{2+} as 1:1 (or 1:1.2). Concentration of components in mass %

precipitate, which, depending on process parameter values (mainly pH) and solution composition, can form various crystal or amorphous phases: $CaHPO_4·2H_2O$ (brushite, DCPD), $Ca_4H(PO_4)_3·2.5H_2O$ (OCP), $Ca_3(PO_4)_2·nH_2O$ (ACP or TCP, n may be also 0), $Ca_5(PO_4)_3OH$ (hydroxyapatite, HAP) and other ones (Valsami-Jones 2001). Effect of calcium ions on struvite reaction crystallization course and product quality was presented elsewhere by Le Corre (batch reaction crystallization—Le Corre et al. 2005) and Hutnik (continuous reaction crystallization—Hutnik et al. 2011, 2017). Presence of calcium ions in cattle liquid manure represents mixture of struvite and calcium phosphates(V) (Hutnik et al. 2013; Kozik et al.2014a b, c, 2015, 2016), what essentially influences utilization of this product as a mineral fertilizer (Latifian et al. 2012). Also hydroxides and salts of selected impurities present in CLM can be identified in a product (Kozik et al. 2015, 2016). Size distributions of these multicomponent products depend mainly on composition of cattle liquid manure and continuous reaction crystallization process parameters (Le Corre et al. 2009; Kozik et al. 2014b). From the authors' earlier research studies and analysis it is seen that the sizes of struvite product crystal vary in relatively broad range: from few up to more than 200 μm (Kozik et al. 2015, 2016).

The experimental test results with appropriate kinetic calculations, concerning continuous reaction crystallization of sparingly soluble phosphates(V) from cattle liquid manure (CLM) in a continuous laboratory DT MSMPR (Draft Tube, Mixed Suspension Mixed Product Removal) crystallizer with internal circulation of suspension driven by propeller stirrer are presented. Crystallizer was provided with the feed prepared from the real CLM, however, artificially enriched under laboratory conditions in other nutrients (correction of composition) and in magnesium ions (for struvite synthesis reaction the PO_4^{3-}: Mg^{2+} proportions were set as 1:1 and 1:1.2). From crystal size distributions of the products nucleation rates B and linear crystal growth rates G of struvite were estimated. Two kinetic models derived for continuous mass crystallization in MSMPR crystallizer were employed: SIG (Size Independent Growth) (Mullin 1993; Randolph and Larson 1988) and RE SDG (Rojkowski Exponential Size Dependent Growth) model (Rojkowski 1977; Koralewska et al. 2009). Knowledge of these continuous processes kinetics may be especially useful for elaboration of technology of phosphates(V) recovery from cattle liquid manure. Since literature provides usually rather batch struvite reaction crystallization experiments results, data from continuous tests are hardly ever accessible in literature. Experimentally verified kinetic data may be useful in design of continuous phosphorus recycling plants comply with Industry 4.0 standards, goals and principles.

Theoretical

For steady state mass crystallization process in a continuous crystallizer with perfectly mixed suspension and removal of unclassified, representative product (abbreviated as ideal MSMPR crystallizer) crystal population balance can be presented in a form of the following differential Equation (1) (Randolph and Larson 1988):

$$-\frac{dn(L)}{n(L)} = \frac{dL}{G(L)\tau} + \frac{dG(L)}{G(L)}, \tag{1}$$

where $n(L)$ is population density for crystal size L, $G(L)$ is linear growth rate corresponding to size L and τ is mean residence time of crystal suspension in a crystallizer.

Equation (1) results from the following simplifying assumptions:

$$-\int_{n_0}^{n} \frac{dn}{n(L)} = \int_{0}^{L} \frac{dL}{G(L)\tau} + \int_{G_0}^{G} \frac{dG(L)}{G(L)}, \tag{4}$$

As a specific $G(L)$ relation the Rojkowski exponential kinetic model (RE SDG) (5) was assumed (Rojkowski 1977). It is one of two SDG kinetic models reliably fitting the experimental data concerning continuous reaction crystallization of struvite (Koralewska et al. 2009):

$$G(L) = G_\infty - (G_\infty - G_0)\exp(-aL), \tag{5}$$

where G_∞ is maximal linear crystal growth rate (of the largest crystals), G_0 is minimal linear crystal growth rate (of nuclei $L=0$) and a is empirical parameter.

Solving of Eq. (4) supplemented with detailed (5) $G(L)$ dependency provides one with analytical solution—$n(L)$ function (6) (Machej and Piotrowski 2001):

$$n = n_0 \exp\left[-\left(\ln\frac{G_\infty - (G_\infty - G_0)\exp(-aL)}{G_0}\left[\frac{1}{G_\infty a\tau} + 1\right] + \frac{L}{G_\infty \tau}\right)\right] \tag{6}$$

- all crystals are geometrically similar,
- crystals aggregation, agglomeration, attrition and disruption phenomena do not occur,
- crystal size distribution can be approximated with continuous function (very large number of crystals),
- nuclei formed in a crystallizer have zero size,
- no crystals in a feed.

Assuming that McCabe rule is fulfilled, thus crystal growth rate G does not depend on crystal size ($G(L)=G=$const. for a given supersaturation), Eq. (1) simplifies further to (2):

$$G\frac{dn(L)}{dL} + \frac{n(L)}{\tau} = 0 \tag{2}$$

Equation (2) represents the commonly used kinetic model abbreviated as SIG model. From (2) one can derive population density distribution function $n(L)$ of solid product (3):

$$n(L) = n_0 \exp\left(-\frac{L}{G\tau}\right), \tag{3}$$

where n_0 is nuclei population density (n for $L=0$).

Equation (3) is used for experimental data fitting and calculation—for the known mean residence time of suspension in a crystallizer τ—linear crystal growth rate G and nucleation rate $B=n_0G$ (Mullin 1993).

Contrarily, considering in crystal population balance (1) crystal growth rate dependent on their sizes ($G(L)\neq$const., SDG model) requires assumption of some specific form of $G(L)$ dependency, followed by solving the resulting Eq. (4):

Knowing the nuclei population density, n_0, and their linear growth rate, G_0 (or one G value independent of size for SIG model), nucleation rate B can be calculated with the following relation (7a—for SDG kinetics or 7b—for SIG kinetics):

$$B = n_0 G_0 \tag{7a}$$

$$B = n_0 G \tag{7b}$$

Experimental

Photo of the experimental plant is presented in Fig. 1a. It is fully programmed and automated Mettler Toledo plant. Steering, control and acquisition of measurement data were done with the use of PC computer (driven by iControl LabMax 4.0 software). The investigated continuous process ran in DT MSMPR type crystallizer of working volume V_w 0.6 dm³ (total volume V_t 2.0 dm³) (Kozik et al. 2015).

Details of research laboratory-scale plant are presented in its schematic diagram—Fig. 1b. Crystallizer unit (adapted automatic reactor LabMax Mettler Toledo), made of the glass, was supplied with heating/cooling jacket working as heat exchanger and stabilizing the predetermined process temperature, as well as in the system providing compressed air necessary for the absorbed CO_2 removal and oxidation of organic substances present in the struvite reaction crystallization environment. Crystallizer diameter was d 100 mm, working part height h_w 70 mm, total height h_t 200 mm.
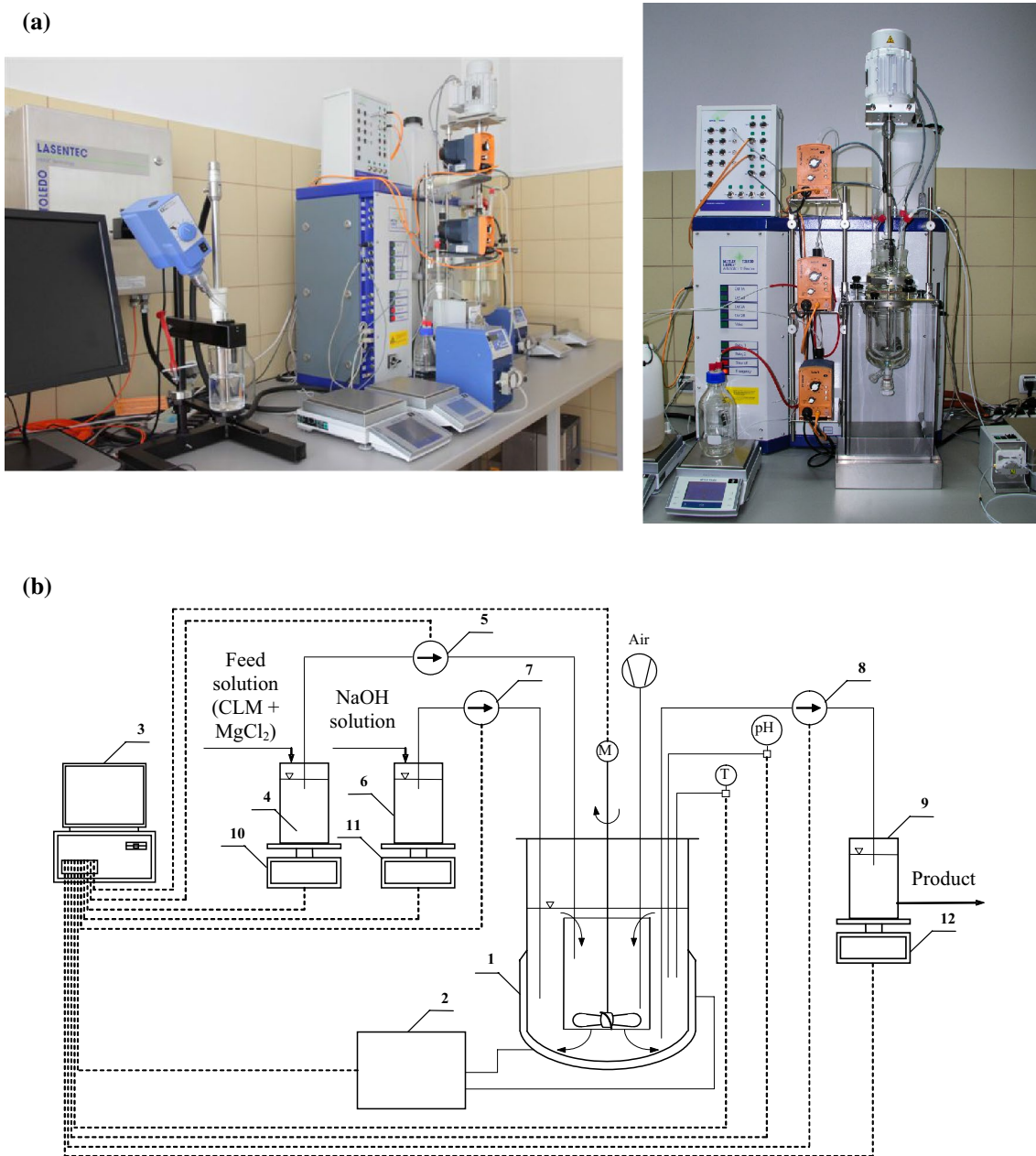
(a)

(b)

Fig. 1 **a** Experimental stand designed for research on continuous reaction crystallization of struvite (Mettler Toledo automatic system). **b** Schematic diagram of the experimental plant: 1—DT MSMPR type crystallizer with internal circulation of suspension, 2—thermostat, 3—PC computer, 4—reservoir of a feed: cattle liquid manure (CLM) and MgCl$_2$, 5—feed proportioner (pump), 6—alkalinity agent tank: aqueous solution of NaOH, 7—proportioner (pump) of NaOH solution, 8—receiver (pump) of product crystal suspension from the crystallizer tank, 9—storage tank of a product crystal suspension, 10, 11, 12—electronic balances, Air—compressed air delivery system, *M*—stirrer speed control/adjustment, pH—alkaline/acid reaction control/adjustment, *T*—temperature control/adjustment

Inside crystallizer unit the circulation profile element (DT, draft tube, d_{dt} 54 mm, h_{dt} 45 mm) was installed, holding 4-paddle propeller mixer of diameter d_m 46 mm. Mixer speed, process temperature, compressed air stream, feed and pH correction solution inflows and product crystal suspension outflow from the crystallizer were rigorously controlled and adjusted when appropriate by computer.

Feed was provided directly into circulation pipe (DT) sub-volume (mixer speed: 4.0 1/s; suspension movement towards bottom). Into annular space outside DT element (suspension movement to the top) aqueous sodium hydroxide solution (3 mass% NaOH) was precisely injected stabilizing and correcting the predetermined pH 8.5 or 9. Constant process temperature 298 K was assumed. Volumetric flow rate

of the feed was 2.4 or 0.6 dm³/h; in effect mean residence times of suspension in a crystallizer were 900 or 3600 s, appropriately. After predetermined parameter stabilization, steady-state process ran through five mean residence times. After each steady-state test solid-phase content in suspension (M_T) was determined and suspension was separated into solid and liquid fraction on a vacuum filter. Solid product was not washed with water. Instead, it was dried "as is" in ambient air.

Cattle feaces and urine were sampled in a cattle breeding animal farm near Wroclaw, Poland (collective tank), and then carefully premixed and filtered. In a dark brown, nearly black filtrate one could clearly observe suspended small particles (fines) of the solid phase. On the free surface of filtrate some stable foam self-formed. Its pH demonstrated alkaline character (pH 9.16). From the chemical composition analysis it resulted that simultaneous action of preprocessing time (starting from „formation" up to filtration and chemical analysis) significantly exceeded the corresponding induction time (unknown for this system). Moreover, alkaline pH of liquid manure/filtrate was responsible for practically total co-precipitation of sparingly soluble species including magnesium and calcium phosphates(V), as well as metal hydroxides. Precipitated salts and hydroxides enriched thus solid phase which was separated during filtration. In effect the original composition of liquid phase was altered significantly. In filtrate, however, neither phosphates(V) nor most of the magnesium, calcium, copper, iron, manganese, molybdenum and zinc ions were observed. Chemical composition of liquid manure was thus purposefully adjusted in laboratory conditions (restoring back its starting composition). However, the literature values of individual components concentrations (Sommer et al. 2013; Rahman et al. 2014) were assumed. Also chemical composition of so-called "synthetic liquid manure" together with experimental results presented in Kozik et al. (2014b) was considered. Obtained this way, "new liquid manure" solution was prepared in external mixer, based on the following substances in crystalline form: $NH_4H_2PO_4$, $MgCl_2 \cdot 6H_2O$, NaCl, $CaCl_2$, $CuCl_2 \cdot 2H_2O$, $MnCl_2 \cdot 4H_2O$, $ZnCl_2$ together with $FeCl_3 \cdot 6H_2O$ (analytically pure, POCh, Gliwice, Poland), standard solution $(NH_4)_6Mo_7O_{24}$ (CertiPUR, Merck, Germany) and deionized water (Barnstead-NANOpure DIamond).

Crystallizer was continuously provided with a feed representing filtrate of cattle liquid manure with complemented (restored) chemical composition and enriched in magnesium ions—substrate in struvite reaction crystallization process. Detailed chemical composition of the crystallizer feed is shown in Table 1 (for molar proportion PO_4^{3-} : Mg^{2+} in a feed set as 1:1 and 1:1.2).

After stabilization of the predetermined parameter values in a crystallizer (T 298 K, pH 8.5 or 9, τ 900 or 3600 s), process additionally ran in a steady state through the time
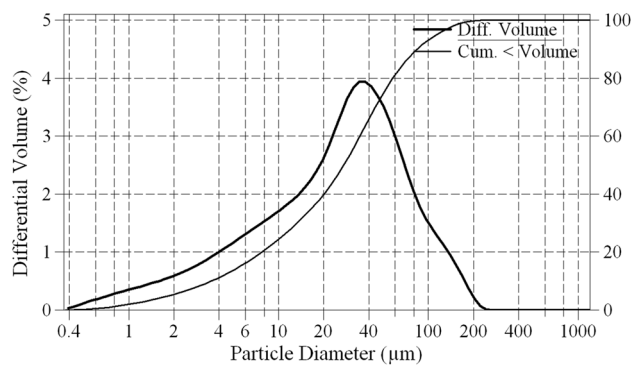

Fig. 2 Exemplary differential (left scale) and cumulative (right scale) volumetric (mass) crystal size distributions of product particles. Process parameters: T 298 K, pH 9, τ 3600 s. Product particles: maximal size L_{max} 220 µm, $L < 5$ µm: 13.8%, mean size L_m 37.0 µm, mode size L_d 38.0 µm, coefficient of crystal size variation CV 97.5% (Kozik et al. 2015)

equivalent of five mean residence times (thus 4500 s or 18,000 s). After this time solid-phase content in suspension (M_T) was determined. Then suspension was directed to vacuum filter. Solid phase, after mechanical separation of mother liquor, was not water washed. Instead, product was dried in air in ambient temperature.

Chemical compositions of mother liquor and solid product were determined with atomic absorption spectrometer iCE 3000 (metals), spectrophotometer UV–VIS Evolution 300 [phosphates(V)] and by titration method (ammonium, formalin method). The powder samples with addition of melt—lithium borates mixture were melted and subjected to chemical analysis (phosphorus and metals) by means of X-ray fluorescence spectrometer PANalytical Magi'X PW2424. Quantitative chemical composition based on calibration dependencies and ZAF correction equations was determined according to international standard PN EN ISO 12,677: 2011.

The X-ray tests were done in Certified Laboratory in Institute of Ceramics and Building Materials in Gliwice (Poland) (http://icimb.pl/gliwice/).

The PANalytical XPERT PRO MPD X-ray diffractometer, equipped with an X-ray tube with a Cu anode, an X'Celerator RTMS detector and sample spinner was used in the investigations reported in the work. Experimental conditions were individually selected according to the specific sample character. The most often X-ray pattern for phase analysis in angular range 5–80° 2θ was collected with tube settings 40 kV and 30 mA.

Qualitative phase analysis by means of PANalytical High-Score software and ICDD PDF 4+ database was carried out. Quantitative phase composition analyses by standardless Rietveld method using Siroquant software were determined.

Table 2 Characteristics of solid Particle size distribution parameters (CLM) in continuous reaction crystallization

No.	Process parameters			Particles produced from cattle liquid manure			
	pH (−)	τ (s)	PO_4^{3-}: Mg^{2+} **	L_m (µm)	L_{50} (µm)	L_d (µm)	CV (%)
1	8.5	900	1:1	17.8	15.1	28.7	78.8
2	9	900	1:1	12.4	7.7	8.5	101.0
3	9	3600	1:1	37.0	27.2	38.0	97.5
4	9	3600	1:1.2	40.2	29.6	39.8	98.8

Process temperature: 298 K (Kozik et al. 2015, 2016)

Average solid-phase content in a product suspension: M_T 8.8 kg_{solid} m^{-3}

L_m—mean crystal size, $L_m = \Sigma x_i L_i$, where: x_i—mass fraction of crystals of mean fraction size L_i; L_{50}—median crystal size for 50 mass % undersize fraction in cumulative distribution; L_d—crystal mode size; $CV = 100(L_{84}—L_{16})/(2L_{50})$, where: L_{84}, L_{16}, L_{50}—crystal sizes corresponding to: 84, 16 and 50 mass % undersize fractions in cumulative distribution

*After drying, without water washing of solid phase on a filter

**Molar ratio in a feed

Table 3 Product phase composition (Kozik et al. 2015, 2016)

Component	Content (in mass %) for molar ratio PO_4^{3-}: Mg^{2+} as:	
	1: 1	1: 1.2
Struvite, $MgNH_4PO_4 \cdot 6H_2O$	58.6 ± 0.2	62.2 ± 0.2
Amorphous phase	36.2 ± 0.6	33.4 ± 0.6
Halite, NaCl	3.6 ± 0.1	3.2 ± 0.1
Sylvite, KCl	1.6 ± 0.1	1.2 ± 0.1

T 298 K, pH 9, τ 3600 s

Table 4 Chemical composition of solid phase produced from cattle liquid manure (CLM) in continuous reaction crystallization process

Component	Content (in mass %) for molar ratio PO_4^{3-}: Mg^{2+} as:	
	1: 1	1: 1.2
P_2O_5	29.61	28.32
MgO	11.27	13.11
CaO	12.03	9.16
Fe_2O_3	0.05	0.06
K_2O	2.49	2.38
MnO	0.25	0.24
Na_2O	3.83	3.66
Others	0.09	0.04
Weight loss during drying in temperature 378 K + weight loss during roasting in temperature 1298 K	43.12	40.39

T 298 K, pH 9, τ 3600 s

Using solid particle laser analyzer Beckman Coulter LS 13,320, size distributions of product particles and their statistical parameters were determined. Particle shapes were evaluated based on computer-aided analysis of images provided by scanning electron microscope JEOL JSM 5800LV.

Differential thermal analysis DTA, thermogravimetry TG and differential thermogravimetry DTG were carried out using STA 409 PC Netzsch thermal analyser equipped with quadrupole mass spectrometer QMS 403 C Aëolos for evoluted gas phase analysis (EGA). The apparatus worked at temperature range 20–1450 °C and allowed for analysis in corundum or platinum crucibles. As reference materials corundum was used.

From CLM of composition presented in Table 1, solid product was manufactured whose sample is shown in Fig. 2.

Statistical parameters of particle size distributions covering all manufactured products discussed in this study are presented in Table 2. Depending on the process parameter values, these were particles of size L_m from 12.4 µm (pH 9, τ 900 s, PO_4^{3-}: Mg^{2+} as 1:1) to 40.2 µm (pH 9, τ 3600 s, PO_4^{3-}:Mg^{2+} as 1:1.2) representing, however, unsatisfactory homogeneity: CV 101.0% and 98.8%, appropriately. Mode size L_d of these product populations varied within the 8.5–39.8 µm range.

Phase compositions of the products are presented in Table 3. These compositions were determined using X-ray tests (X-ray diffractometer).

It was concluded that product contained from 58.6 to 62.2 mass % of struvite $MgNH_4PO_4 \cdot 6H_2O$ depending on molar ratio of PO_4^{3-} to Mg^{2+} in a crystallizer feed point. Also crystalline halite NaCl (3.2–3.6 mass %) and sylvite KCl (1.2–1.6 mass%) were identified. Some amorphous phase (33.4–36.2 mass %) was observed, as well. Comparing the quantitative phase analysis results (Table 3) with the feed composition (Table 1) one must conclude that amorphous phase is composed mainly of hydrated forms of some calcium phosphates(V) (Valsami-Jones 2001). One can also expect that co-precipitating sparingly soluble hydroxides of some metal impurities were present in this phase, as well.

Chemical composition of solid phase, determined with the use of X-ray fluorescence spectrometer, is presented in

Table 5 Nucleation rate B and crystal linear growth rate G values estimated for struvite continuous reaction crystallization process from cattle liquid manure (CLM) in DT MSMPR crystallizer

No.	Process kinetic parameters values—SIG MSMPR model			
	$n(L)$ for $L > 50$ µm	n_0 (m^{-1} m^{-3})	G (µm s^{-1})	B (s^{-1} m^{-3})
1	$n = 1.162 \times 10^{17} \exp(-1.100 \times 10^5\, L)$	1.2×10^{17}	1.01×10^{-2}	1.2×10^9
2	$n = 3.330 \times 10^{18} \exp(-2.183 \times 10^5\, L)$	3.3×10^{18}	5.09×10^{-3}	1.7×10^{10}
3	$n = 2.221 \times 10^{16} \exp(-6.759 \times 10^4\, L)$	2.2×10^{16}	4.11×10^{-3}	9.0×10^7
4	$n = 1.395 \times 10^{16} \exp(-5.763 \times 10^4\, L)$	1.4×10^{16}	4.82×10^{-3}	6.7×10^7

Kinetic parameters calculated with SIG MSMPR model [Eq. (3)]. Process conditions—see Table 2

Table 6 Nucleation rate B, linear (minimal) growth rate of nuclei G_0 and maximal linear growth rate of crystals G_∞ values estimated for continuous struvite reaction crystallization process from cattle liquid manure (CLM) in DT MSMPR crystallizer

No.	Process kinetic parameters values—RE SDG MSMPR model				
	n_0 (m^{-1} m^{-3})	G_0 (µm s^{-1})	G_∞ (µm s^{-1})	a (µm^{-1})	B (s^{-1} m^{-3})
1	1.82×10^{26}	9.81×10^{-6}	1.02×10^{-2}	0.048391	1.78×10^{15}
2	2.99×10^{26}	6.46×10^{-6}	8.48×10^{-3}	0.065918	1.93×10^{15}
3	1.04×10^{24}	9.20×10^{-6}	5.30×10^{-3}	0.025007	9.57×10^{12}
4	3.09×10^{23}	1.82×10^{-5}	5.52×10^{-3}	0.021000	5.62×10^{12}

Kinetic parameters calculated with RE SDG MSMPR model [Eqs. (5) and (6)]. Process conditions—see Table 2

Table 4. More thorough analysis of component concentrations in a crystallizer feed, in mother liquor and in solid product was presented elsewhere (Kozik et al. 2015, 2016).

Results and discussion

Based on analysis of experimental population density distributions of the solids produced from cattle liquid manure (CLM) (particle size distribution parameters—see Table 2) it was concluded that for struvite crystals of size $L > 50$ µm the $n(L)$ dependency may be approximated with linear function (in ln$n$—L coordinates). From SIG MSMPR kinetic model the linear crystals' growth rate G and nucleation rate B were determined. Regression parameters of population density distribution function (3) valid for struvite crystals of size $L > 50$ µm and calculated on this basis G and B values are presented in Table 5.

Practical applicability range of SIG MSMPR model in experimental $n(L)$ data fitting (linearity in ln n-L system) for $L > 50$ µm only made, that kinetic parameter values calculated with this model have limited practical implementation. These may be useful only for, e.g. the test results comparison. This especially concerns the nuclei population densities n_0 and n_0-dependent nucleation rates B. From the analysis and comparison of kinetic parameters (Table 2 and 5) it results that slight rise of pH from 8.5 to 9 (for τ 900 s) produced that G decreased as much as 2-times, whereas B enlarged more than 14-times. Mean product crystal size decreased from L_m 17.8 to 12.4 µm, whereas population's size-homogeneity, as CV, also
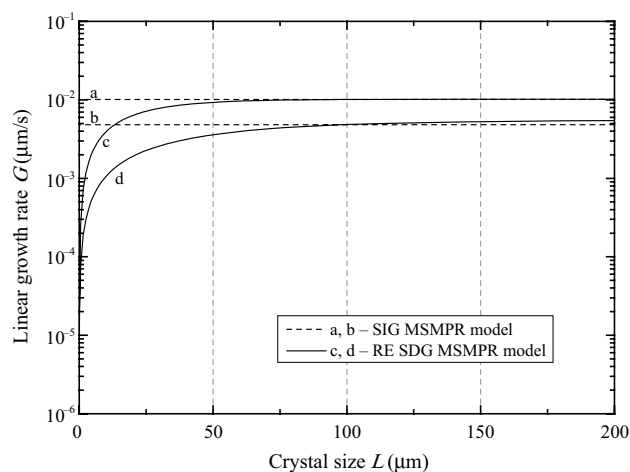

Fig. 3 Size-dependence of linear growth rate of struvite crystals in DT MSMPR crystallizer. General comparison of predictions with Eqs. (3) (5) and (6) and kinetic data from Tables 5 and 6: a and b—SIG MSMPR model; c and d—RE SDG MSMPR model. Process parameters: pH 8.5, τ 900 s, PO$_4^{3-}$: Mg^{2+} = 1:1—lines a and c; pH 9, τ 3600 s, PO$_4^{3-}$: Mg^{2+} = 1:1.2—lines b and d

distinctly decreased (CV above 100%) (Table 2). Elongation of mean residence time of suspension in a crystallizer up to τ 3600 s made that nucleation rate decreased from 1.7×10^{10} to 9.0×10^7 s^{-1} m^{-3} (nearly 190-times). Linear growth rate G also slightly decreased; however, elongated contact time of struvite crystals with supersaturated mother liquor made that final product size raised (L_m enlarged up to 37.0 µm). Magnesium ions excess in relation to phosphate(V) ions' concentration (as 1.2:1)

influenced the particle sizes advantageously. Mean size of struvite crystals L_m enlarged by more than 8%, owing to simultaneously both higher linear struvite crystal growth rate (4.82×10^{-3} μm s^{-1}) and lower nucleation rate (6.7×10^7 s^{-1} m^{-3}) (Table 5).

Employing of the same experimental data $n(L)$ for kinetic calculations, but assuming validity of the RE SDG MSMPR model frame, leads up to different kinetic parameter values (Table 6).

The assumed more complex SDG model renders characteristic curvature of $n(L)$ in ln n-L coordinates very well (Hutnik et al. 2013; Kozik et al. 2014b). Thus, the calculated G_0, G_∞ and B parameter values may be with high probability regarded as reliable for description and kinetic modelling of struvite continuous reaction crystallization from cattle liquid manure. Effect of process parameters changes (Table 2) on the n_0, $G_{(0,\infty)}$ and B parameter change trends is generally identical with the results corresponding to simpler SIG MSMPR model (3) (presented above) (compare Table 5 with Table 6). The most advantageous conditions for crystalline struvite production corresponded to pH 9, τ 3600 s and 20% magnesium ions' excess in relation to phosphate(V) ions concentration. These represent the lowest nuclei population density n_0 (3.09×10^{23} m^{-1} m^{-3}), the highest linear growth rate of nuclei G_0 (1.82×10^{-5} μm s^{-1}) at the smallest nucleation rate B (5.62×10^{12} s^{-1} m^{-3}). In result mean size of struvite crystals in a product was 40.2 μm.

Comparison of simulated linear struvite crystal growth rates, calculated with both kinetic models: SIG and RE SDG is presented in Fig. 3.

Linear growth rate of struvite crystals predicted by SIG MSMPR model is constant, independent of crystal size. Exemplary G values from SIG MSMPR—demonstrated in Fig. 3 as horizontal lines a and b—are 1.01×10^{-2} and 4.82×10^{-3} μm s^{-1} for the process parameters shown in Table 2 (see No. 1 and 4, respectively). For the same process parameter sets, graphical courses of $G(L)$ dependencies (c and d lines) predicted by RE SDG MSMPR model (Eq. (5), see No. 1 and 4 in Table 6) are also presented in the same Fig. 3. With the rise of struvite crystal sizes, linear growth rate nonlinearly increases from initial nuclei growth rate G_0 (9.81×10^{-6} μm s^{-1}—c line; 1.82×10^{-5} μm s^{-1}—d line) for the crystals of size $L = 0$, up to maximal G_∞ values 1.02×10^{-2} and 5.52×10^{-3} μm s^{-1}, correspondingly. However, for the crystals of size larger than ca. 50 μm, linear growth rate $G(L)$ stabilizes and becomes practically constant. Analysing these observations it results that in continuous reaction crystallization system, especially in the cattle liquid manure environment, the struvite crystals grow at different rates. Small crystals grow slower, and larger ones—faster. One should also notice, that the G values calculated with the most simplified SIG kinetic model (3) are

rather for struvite crystals of larger sizes, similar to G_α values predicted with the selected, more flexible SDG model (6). In some cases (see line a and c in Fig. 3) these are even practically identical. It is important process observation for the detailed analysis of struvite reaction crystallization from cattle liquid manure in the continuous operation mode.

It may be generally concluded that changes in decisive parameters of continuous struvite reaction crystallization process (pH = 8.5 or 9, τ = 900 or 3600 s and PO$_4$$^{3-}$: Mg^{2+} = 1:1 or 1:1.2) produced qualitatively similar—increasing or decreasing—trends in nuclei population density n_0 of struvite, in linear growth rate of its crystals G and in nucleation rate B values calculated with both kinetic models. It should be noticed, however, that the n_0 and B values calculated with both kinetic models are not comparable directly; the differences can reach even 10^5–10^6. It results from significant simplifications in SIG MSMPR model which was constrained only to linear data extrapolation for lower sizes. However, linear growth rates of struvite crystals G (SIG MSMPR model) and G_∞ (RE SDG MSMPR model) are similar.

Conclusions

Kinetic parameters of continuous struvite reaction crystallization process from cattle liquid manure (CLM) were estimated. Calculations involved two kinetic model frames, both valid for ideal continuous MSMPR crystallizer: SIG and RE SDG. Especially low pH (8.5), elongated mean residence time of suspension in a crystallizer (3600 s) and magnesium ions excess in relation to phosphate(V) ions' concentration (1.2:1) favour the process effects in respect to product crystal quality. Besides B, the G and G_∞ may be regarded as moderately reliable data for struvite continuous reaction crystallization kinetics modelling in the considered process conditions (cattle liquid manure—CLM): G from 4.11×10^{-3} to 1.01×10^{-2} μm s^{-1} and G_∞ from 5.30×10^{-3} to 1.02×10^{-2} μm s^{-1}. Presented, experimentally verified kinetic data can be employed in analysis of continuous process variant. Continuous mode complíes with Industry 4.0 standards, goals and principles (however, which kinetic data are hardly ever met in accessible literature) makes integration of reaction crystallization process with other, the most often also continuous unit operations within the whole plant possible. Moreover, continuous mode of reaction crystallization process provides stable process conditions and thus related stable product properties. One can suppose that, because of growing phosphorus recycling scale, continuous operation mode will dominate in nearest future and experimental data related to continuous approach may find them useful in industrial practice.

Compliance with ethical standards

Conflict of interest On behalf of all authors, the corresponding author states that there is no conflict of interest.

References

Hutnik N, Piotrowski K, Wierzbowska B, Matynia A (2011) Continuous reaction crystallization of struvite from phosphate(V) solutions containing calcium ions. Cryst Res Technol 46:443–449. https://doi.org/10.1002/crat.201100049

Hutnik N, Kozik A, Mazienczuk A, Piotrowski K, Wierzbowska B, Matynia A (2013) Phosphates(V) recovery from phosphorus mineral fertilizers industry wastewater by continuous struvite reaction crystallization process. Wat Res 47:3635–3643. https://doi.org/10.1016/j.watres.2013.04.026

Hutnik N, Stanclik A, Matynia A (2017) Influence of calcium ions on struvite precipitation and crystallization from wastewaters. Przem Chem 96:1864–1868. https://doi.org/10.15199/62.2017.9.8

Koralewska J, Piotrowski K, Wierzbowska B, Matynia A (2009) Kinetics of reaction-crystallization of struvite in the continuous draft tube magma type crystallizers—influence of different internal hydrodynamics. Chin J Chem Eng 17:330–339. https://doi.org/10.1016/S1004-9541(08)60212-8

Kozik A, Hutnik N, Mazienczuk A, Wierzbowska B, Piotrowski K, Podwórny J, Matynia A (2014a) Phosphates(V) recovery from synthetic liquid manure by continuous struvite reaction crystallization process. In: Proceedings of 41st international conference of SSCHE, Tatranské Matliare, Slovakia, p 853–861. (**ISBN: 978-80-89475-13-1, EAN: 9788089475131**)

Kozik A, Hutnik N, Piotrowski K, Matynia A (2014b) Continuous reaction crystallization of struvite from diluted aqueous solution of phosphate(V) ions in the presence of magnesium ions excess. Chem Eng Res Des. 92:481–490

Kozik A, Hutnik N, Podwórny J, Gerle A, Mazienczuk A, Matynia A (2014c) Recovery of phosphate(V) ions from synthetic swine wastewater under stoichiometric conditions. Przem Chem. 93:559–564. https://doi.org/10.12916/przemchem.2014.559

Kozik A, Hutnik N, Hoffmann K, Huculak-Maczka M (2015) Phosphates(V) ions recovery from cattle manure. Przem Chem 94:938–942. https://doi.org/10.15199/62.2015.6.15

Kozik A, Hutnik N, Piotrowski K, Matynia A (2016) Precipitation of calcium and magnesium phosphates(V) from cattle manure. In: Proceedings of 43rd international conference of SSCHE, Tatranské Matliare, Slovakia, p 508–515. (**ISBN: 978-80-89597-35-2, EAN: 9788089597352**)

Latifian M, Liu J, Mattiasson B (2012) Struvite-based fertilizer and its physical and chemical properties. Environ Technol 33:2691–2697. https://doi.org/10.1080/09593330.2012.676073

Le Corre KS, Valsami-Jones E, Hobbs P, Parsons SA (2005) Impact of calcium on struvite crystal size, shape and purity. J Cryst Growth 283:514–522. https://doi.org/10.1016/j.jcrysgro.2005.06.012

Le Corre KS, Valsami-Jones E, Hobbs P, Parsons SA (2009) Phosphorus recovery from wastewater by struvite crystallization: a review. Crit Rev Environ Sci Technol 39:433–477. https://doi.org/10.1080/10643380701640573

Machej K, Piotrowski K (2001) Review and comparison of kinetic equations for mass crystallization design purposes. Inz Ap Chem 40(5):17–18

Mullin JW (1993) Crystallization. Butterworth-Heinemann, Oxford

Parsons SA (2001) Phosphate precipitation from waste waters—recent scientific and technical developments: struvite (magnesium ammonium phosphates). CEEP Scope Newslett 41:15–22

Rahman MM, Salleh MAM, Rashid U, Ahsan A, Hossain MM, Ra CS (2014) Production of slow release crystal fertilizer from wastewaters through struvite crystallization—A review. Arab J Chem 7:139–155. https://doi.org/10.1016/j.arabjc.2013.10.007

Randolph AD, Larson MA (1988) Theory of particulate processes: analysis and techniques of continuous crystallization, 2nd edn. Academia Press, New York. ISBN 9780323161817

Rojkowski Z (1977) New empirical kinetic equation of size dependent crystal growth and its use. Krist Tech 12:1121–1128

Sommer SG, Christensen ML, Schmidt T, Jensen LS (2013) Animal manure recycling. Treatment and Management. Wiley, New Delhi

Valsami-Jones E (2001) Phosphate precipitation from waste waters—recent scientific and technical developments: calcium phosphate precipitation. CEEP Scope Newsl 41:8–15